Sip1 mediates an E-cadherin-to-N-cadherin switch during cranial neural crest EMT

Crystal D. Rogers, Ankur Saxena, and Marianne E. Bronner

Division of Biology 139-74, California Institute of Technology, Pasadena, CA 91125

The neural crest, an embryonic stem cell population, initially resides within the dorsal neural tube but subsequently undergoes an epithelial-to-mesenchymal transition (EMT) to commence migration. Although neural crest and cancer EMTs are morphologically similar, little is known regarding conservation of their underlying molecular mechanisms. We report that Sip1, which is involved in cancer EMT, plays a critical role in promoting the neural crest cell transition to a mesenchymal state. *Sip1* transcripts are expressed in premigratory/migrating crest cells. After Sip1 loss, the neural crest specifier gene *FoxD3* was abnormally retained in the dorsal neuroepithelium, whereas *Sox10*, which is normally required for emigration, was diminished. Subsequently, clumps of adherent neural crest cells remained adjacent to the neural tube and aberrantly expressed E-cadherin while lacking N-cadherin. These findings demonstrate two distinct phases of neural crest EMT, detachment and mesenchymalization, with the latter involving a novel requirement for Sip1 in regulation of cadherin expression during completion of neural crest EMT.

Introduction

The epithelial-to-mesenchymal transition (EMT), whereby epithelial cells become individual mesenchymal cells, is a common feature of embryonic development (Nieto, 2011) and is reiterated during tumor metastasis in adults (Thiery et al., 2009). During this process, profound changes occur in cell morphology such that tightly adherent and polarized epithelial cells are transformed into loosely organized, nonpolarized, and often migratory mesenchymal cells. The cell biological processes underlying EMT have been best studied in cancer cells grown in vitro, and several transcription factors, including *Snail*, *Twist*, and *Sip1/Zeb2/ZFHX1B* (here referred to as Sip1), have been identified as important mediators of EMT in metastasis (Kang and Massagué, 2004; Thiery et al., 2009; Kerosuo and Bronner-Fraser, 2012).

The neural crest (NC) provides a good model system for studying the molecular mechanisms underlying EMT in a nonmalignant environment. Neural crest progenitors first express definitive specification markers, including EMT genes like *Snail2*, in the dorsal midline of the neural tube before initiating emigration in amniotes (Nieto et al., 1994). Shortly thereafter, NC cells commence EMT and subsequently migrate to distant sites where they differentiate into numerous derivatives. Despite the similarities in morphology and gene expression between embryonic and cancer cells undergoing EMT, little is known about the functional conservation of the underlying molecular pathways.

During the process of neural crest EMT, the expression and cellular localization of adhesion molecules such as cadherin 6B (Cad6B) and neural cadherin (Ncad) are highly regulated (Kerosuo and Bronner-Fraser, 2012). Ncad is expressed throughout the apical portion of the neuroepithelium (Akitaya and Bronner-Fraser, 1992) but is down-regulated in trunk dorsal neural tube cells by the NC specifier gene *FoxD3*, allowing EMT to occur (Cheung et al., 2005; Dady et al., 2012). In cancer cells, the process of EMT is highly regulated by a switch between the expression of epithelial cadherin (Ecad) and Ncad, which is up-regulated in migratory mesenchymal cells (Kuphal and Bosserhoff, 2006) and is a common marker of the mesenchymal phenotype (Theveneau et al., 2010). Intriguingly, expression of Ecad recently has been reported in the neural tube and early emigrating NC cells in developing embryos, suggesting that it may play a previously unrecognized role in neural

Correspondence to Marianne E. Bronner: mebronner@gmail.com

Abbreviations used in this paper: Cad6B, cadherin 6B; ContMO, control morpholino oligomer; Ecad, epithelial cadherin; EMT, epithelial-to-mesenchymal transition; HH, Hamburger Hamilton; memRFP, membrane-bound RFP; NC, neural crest; Ncad, neural cadherin; nucRFP, nuclear-targeted RFP; Sip1, Smad-interacting protein 1; Sip1MO, Sip1 translation-blocking control morpholino oligomer.

© 2013 Rogers et al. This article is distributed under the terms of an Attribution–Noncommercial–Share Alike–No Mirror Sites license for the first six months after the publication date (see http://www.rupress.org/terms). After six months it is available under a Creative Commons License (Attribution–Noncommercial–Share Alike 3.0 Unported license, as described at http://creativecommons.org/licenses/by-nc-sa/3.0/).

The Rockefeller University Press $30.00
J. Cell Biol. Vol. 203 No. 5 835–847
www.jcb.org/cgi/doi/10.1083/jcb.201305050

crest EMT (Kuphal and Bosserhoff, 2006; Dady et al., 2012). At midbrain levels, Snail2 directly represses *Cad6B*, which is a prerequisite for EMT progression (Coles et al., 2007). Snail2 functions in a complex with the adaptor protein PHD12 to recruit HDAC to the *Cad6B* promoter (Strobl-Mazzulla and Bronner, 2012). Surprisingly, however, mice that are double mutant for *Snail1* and *Snail2* in the NC do not have an obvious neural crest phenotype (Murray et al., 2007). This result suggests that at least in mice, other EMT mediators may be able to compensate for the lack of *Snail* genes.

One candidate that may compensate for the loss of *Snail2* is the basic helix-loop-helix transcription factor, *Twist*, which is known to have functional redundancy with *Snail2* during mesoderm development in *Drosophila* and mesoderm and NC induction in *Xenopus* (Zhang and Klymkowsky, 2009). In frog, Twist physically interacts with Snail1/2 during NC development (Lander et al., 2013). Twist is post-transcriptionally regulated by an F-box protein, Partner of Paired, which also regulates the levels of other EMT factors, suggesting that there is a conserved mechanism regulating the proteins that control the process of EMT (Lander et al., 2011). In addition, *Twist* has been demonstrated as one of the major factors involved in cancer cell EMT due to its ability to repress the expression of *Ecad* (Kang and Massagué, 2004). However, *Twist* is not highly expressed in the premigratory or migrating NC of amniotes (Bothe et al., 2007) or lamprey embryos (Sauka-Spengler et al., 2007). Moreover, the NC defects observed in *Twist1*-null mice (Chen et al., 2007) appear to be secondarily caused by the loss of *Twist* in the adjacent mesoderm (Chen and Behringer, 1995; Bildsoe et al., 2013). These findings suggest that, in amniotes at least, EMT factors other than *Snail* and *Twist* must be playing an important role in the regulation of NC development.

Another factor implicated in cancer progression and metastasis is Smad-interacting protein 1 (Sip1), which is a two-handed zinc finger transcriptional repressor (Verschueren et al., 1999; Brabletz and Brabletz, 2010). Sip1 has been postulated to play an important role in the transition of epithelial tumors to metastatic cancers (Brabletz and Brabletz, 2010). Similar to the Snail proteins, Sip1 has been shown to directly bind to and repress *Ecad* expression in cancer cells, thus facilitating EMT (Comijn et al., 2001). During embryonic development, Sip1 can function downstream of the BMP signaling pathway as a co-regulator with R-Smad proteins and CtBP, or it can function independent of BMP signaling to repress transcription of its targets (van Grunsven et al., 2007). Although there have been several studies regarding its role in early development (van Grunsven et al., 2000; Sheng et al., 2003; Nitta et al., 2007; Delalande et al., 2008; Lander et al., 2011), little is known about the function of *Sip1* during neural crest EMT.

Here, we examine the role of Sip1 in the transition of neuroepithelial cells to mesenchymal NC cells in avian embryos. The data suggest that neural crest EMT is a two-step process in which cells first detach from the neural tube and then subsequently disassociate from each other to become migratory mesenchymal cells. Our data reveal that, while not required for NC cells to exit the neural tube, *Sip1* is required for cells to become fully mesenchymal, and that their inability to complete EMT in *Sip1*'s absence appears to involve the dysregulation of the adhesion molecules Ecad and Ncad.

Results

Sip1 expression during neurulation and neural crest development

To determine the spatiotemporal pattern of *Sip1* expression during early chick development, we performed whole-mount in situ hybridization. *Sip1* transcripts are barely detectable in the presumptive neural plate at Hamburger Hamilton stage 4 (HH4; Fig. 1 A) but become strongly expressed in this region by HH5 (Fig. 1 B). As neurulation begins, *Sip1* is expressed throughout the neural plate at HH7 (Fig. 1, C and c′). Expression increases at HH8− and HH8, just before neural crest EMT (Fig. 1, D and E). As NC cells begin to emigrate at HH9, *Sip1* expression is maintained in the neural tube and also is present in the newly migratory NC cells (Fig. 1, F and f′). By HH12, *Sip1* is observed in the migratory cranial crest and in the rhombomere 4 migratory stream (Fig. 1, G and g′; arrow), as evidenced by its overlap with the HNK-1 epitope, characteristic of migratory NC cells (Fig. 1 g′, bottom). *Sip1* transcripts are maintained throughout the developing central nervous system and migratory crest at HH12 and HH16 (Fig. 1, G and H), analogous to Sip1 protein expression (Fig. 1 g′′). Taken together, these results show that *Sip1* is expressed throughout early stages of NC development.

Sip1 is required for the acquisition of mesenchymal morphology and completion of cranial neural crest EMT

We tested the functional role of Sip1 in NC development by electroporating a translation-blocking morpholino into the neural plate border region of gastrulating (HH4) embryos, corresponding to the onset of endogenous *Sip1* expression, and examined subsequent effects on neural crest development at HH8–13, corresponding with the expression of neural crest specifier genes and the end of migration in the cranial regions.

At HH8, we examined the effects on expression of the early neural crest specifier gene, *FoxD3*, as well as neural genes, to determine whether the loss of Sip1 affected either neural or neural crest specification. Mulitplex NanoString analysis as well as in situ hybridization at HH8 revealed an early downregulation of *FoxD3* expression after Sip1MO loss, but this decrease appeared to be very transient, recovering by HH9− (Fig. S1, A–D). Similarly, the loss of Sip1 had little or no effect on neural specification, except for a slight change in ERNI at HH8 (Fig. S1, E–I).

Because there appeared to be no prolonged effect on specification, we next examined whether the loss of Sip1 might influence neural crest EMT, which begins at HH9, by examining expression of *FoxD3* and *Sox10*. In embryos lacking Sip1, *FoxD3* expression was abnormally maintained in the dorsal neural tube (Fig. 2, A and a′; $n = 19/33$). At stages when NC cells should be undergoing EMT and leaving the neural tube, the loss of Sip1 also resulted in a decrease in *Sox10* expression (Fig. 2 B; $n = 25/29$), normally required for migration to commence. Demonstrating specificity, we found that co-electroporation of Sip1MO plus mRNA encoding human *Zeb2/Sip1* DNA (Ellis et al., 2010) could partially rescue the loss of *Sox10* expression (Fig. 2 C; $n = 10/21$).

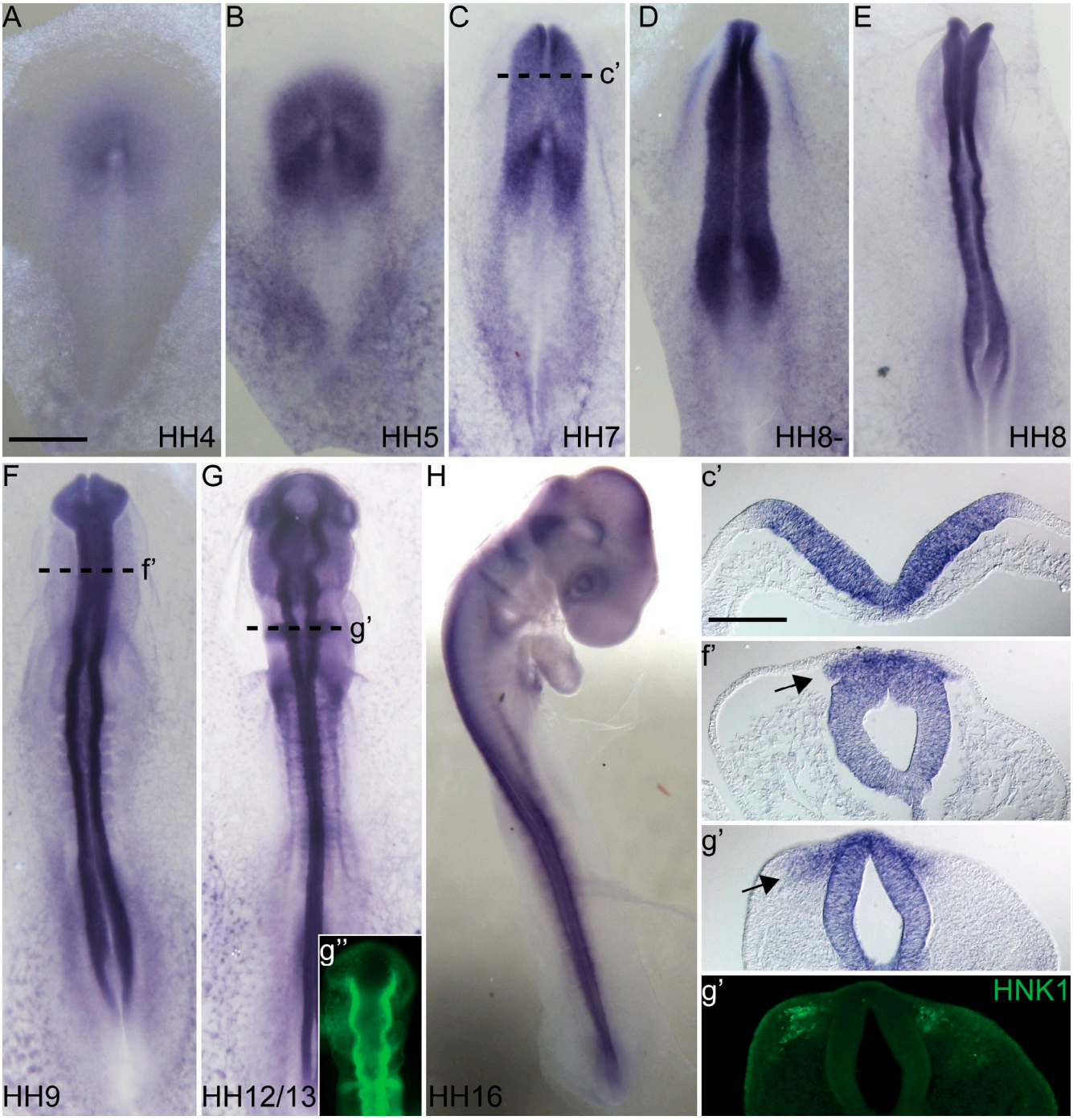

Figure 1. ***Sip1* is expressed in the developing neural and neural crest cells.** (A–H) Whole-mount in situ hybridization of chick embryos at various stages using an antisense probe to *Sip1* reveals expression in the developing neural plate (A–C), neural tube (D–H), and premigratory and migratory NC cells (F–H) at stages HH4–HH16. Sections of embryos at indicated axial level are marked by dashed lines (c′, f′, and g′). *Sip1* is expressed throughout the neural plate, neural tube, and in migratory NC cells (arrow). (g′) Top panel is *Sip1* expression and bottom panel is HNK1 expression in same section showing overlap with migratory cells (arrow). (g′′) Whole-mount immunohistochemistry showing that Sip1 protein is localized to the same tissues as *Sip1* transcript. Bars: (A–H) 200 µm; (c′–g′′)100 µm.

To further explore this phenotype, we examined the expression of Pax7 protein as a nuclear marker for premigratory and early migrating NC cells, and HNK1 as a cell surface marker for migrating NC cells. At HH10, migratory Pax7+ neural crest cells appeared clustered a short distance from the neural tube on the morpholino-injected side compared with the ContMO-injected side of the same embryo, with the latter appearing to have advanced much farther (Fig. 2, D and d′; n = 9/10). HNK1 staining confirmed that Sip1MO-injected cells were indeed able to delaminate from the neural tube but were unable to progress and migrate; instead, they remained attached to each other and/or to the ectoderm (not depicted). Similar

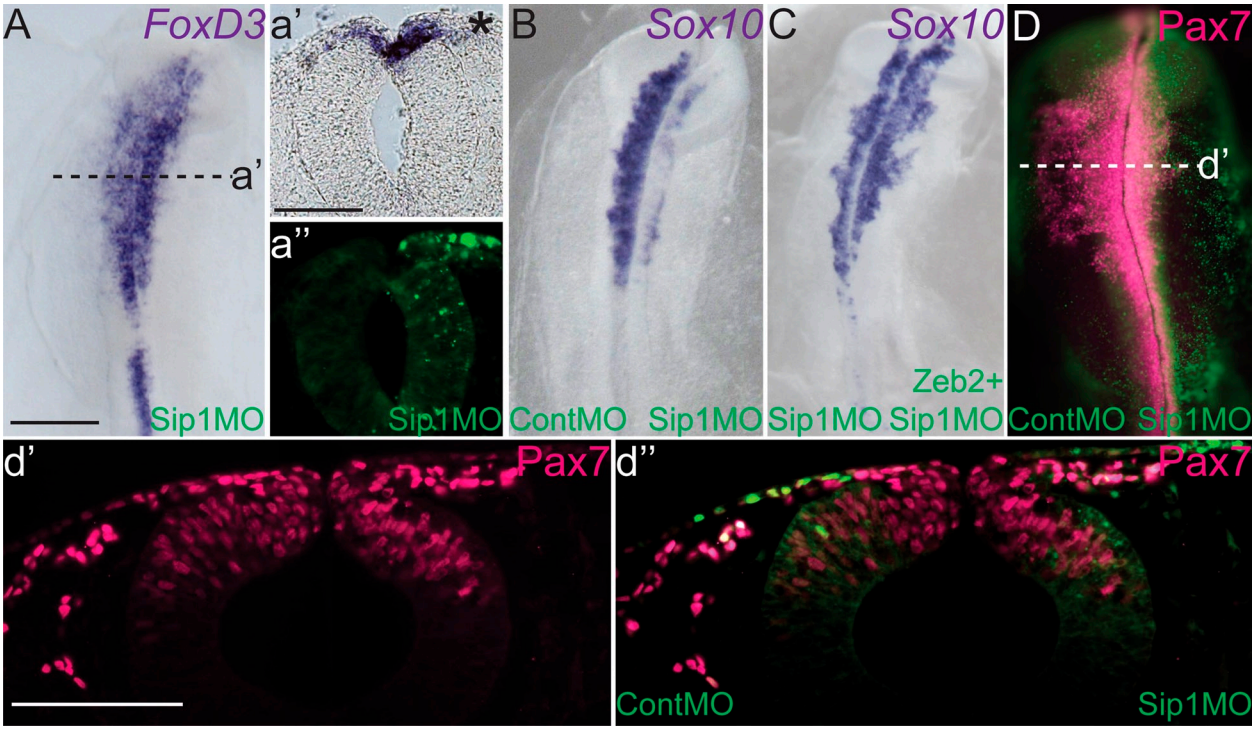

Figure 2. **Loss of Sip1 affects neural crest gene expression.** (A) Whole-mount in situ hybridization with a probe for *FoxD3* in embryos electroporated with Sip1 morpholino (MO) on the right side and analyzed at HH9. A section of an embryo in A showing *FoxD3* expression (a′) after Sip1MO injection marked by FITC (a′′). *FoxD3* is up-regulated on the Sip1MO side (n = 19/33). (B and C) Whole-mount in situ hybridization with a probe for *Sox10* in embryos electroporated with (B) ContMO (left side) and Sip1MO (right side) showing loss of *Sox10* expression (n = 25/29), or (C) Sip1MO (left side) and Sip1MO + Zeb2 DNA showing rescue of that loss (C; n = 10/21). (D) Immunohistochemistry for Pax7 in embryos with ContMO on the left side and Sip1 MO on the right side (green is FITC from ContMO on left and Sip1MO on right). (d′) A section from embryo, in D as indicated by dashed line, showing maintenance of Pax7 expression in premigratory cells but fewer migratory cells (n = 9/10). Right panel is overlay with ContMO and Sip1MO FITC. Bars: (A–d′) 200 µm. The data shown here are from a single representative experiment out of at least three repeats.

phenotypes were observed for electroporations performed at HH4–HH7 (Fig. S2, A and B), though the phenotype was less marked when Sip1 was knocked down at HH7 (Fig. S2 C). Taken together, these data suggest that Sip1-depleted NC cells are able to delaminate from the neural tube but then fail to complete the process of EMT and become mesenchymal cells, as defined by their migratory characteristics.

Embryos were then analyzed by in situ hybridization at stages of active neural crest migration (HH10) for expression of *Sox10* and *FoxD3*, both of which are expressed in migrating neural crest cells. In contrast to control morpholino (ContMO)–injected embryos (Fig. 3, A and C) or the uninjected contralateral side, Sip1 morpholino (Sip1MO)–treated embryos had diminished *Sox10* expression indicative of a reduction in migrating neural crest cells (Fig. 3, B and b′; n = 11/13), while aberrantly maintaining expression of *FoxD3* in the dorsal neural tube (Fig. 3, D and d′; n = 7/10). This suggests an important role for Sip1 in progression of the normal neural crest program. To analyze whether this phenotype persists, embryos were allowed to develop until HH13, by which time cranial NC emigration from the neural tube is complete. Even at these late stages, NC cells remained closely adherent to the dorsal neural tube and ectoderm after Sip1 knockdown (Fig. 3 E; n = 4/5, arrow). The efficiency of Sip1 protein knockdown by the morpholino was verified by Western blot analysis (Fig. 3 F).

To examine this process in the absence of other cell types, cranial neural tubes that were treated with either ContMO or Sip1MO were dissected from HH8 embryos and cultured on fibronectin-coated tissue culture dishes. Immunostaining with the HNK1 antibody demonstrated that the Sip1MO-electroporated neural crest cells were able to separate from the neural tube tissue (Fig. 3 G; n = 8/8; halo of migrating neural crest cells indicated by dotted line) and up-regulate the HNK1 epitope, but unable to individualize and instead remained closely adherent to each other (Fig. 3, compare G–g′ with H–h′). In contrast, NC cells from ContMO explants were highly migratory and displayed mesenchymal cell morphology. Similar to the in vivo findings, these results lend further support to the idea that Sip1 is required for NC cells to complete the process of EMT.

Live imaging of the dorsal neural tube after Sip1 knockdown

To identify the morphological changes that occur in NC cells lacking Sip1 during EMT, we performed live imaging (Videos 1–6). HH4 embryos were electroporated with either FITC-tagged Sip1MO (Video 1) or ContMO (Video 4) along with membrane-localized mem-RFP DNA to better visualize cell shapes and movement. At HH9–10, these embryos were visualized via time-lapse confocal microscopy in order to examine the behavior of cells lacking Sip1 as they exited the neural tube and began migrating.

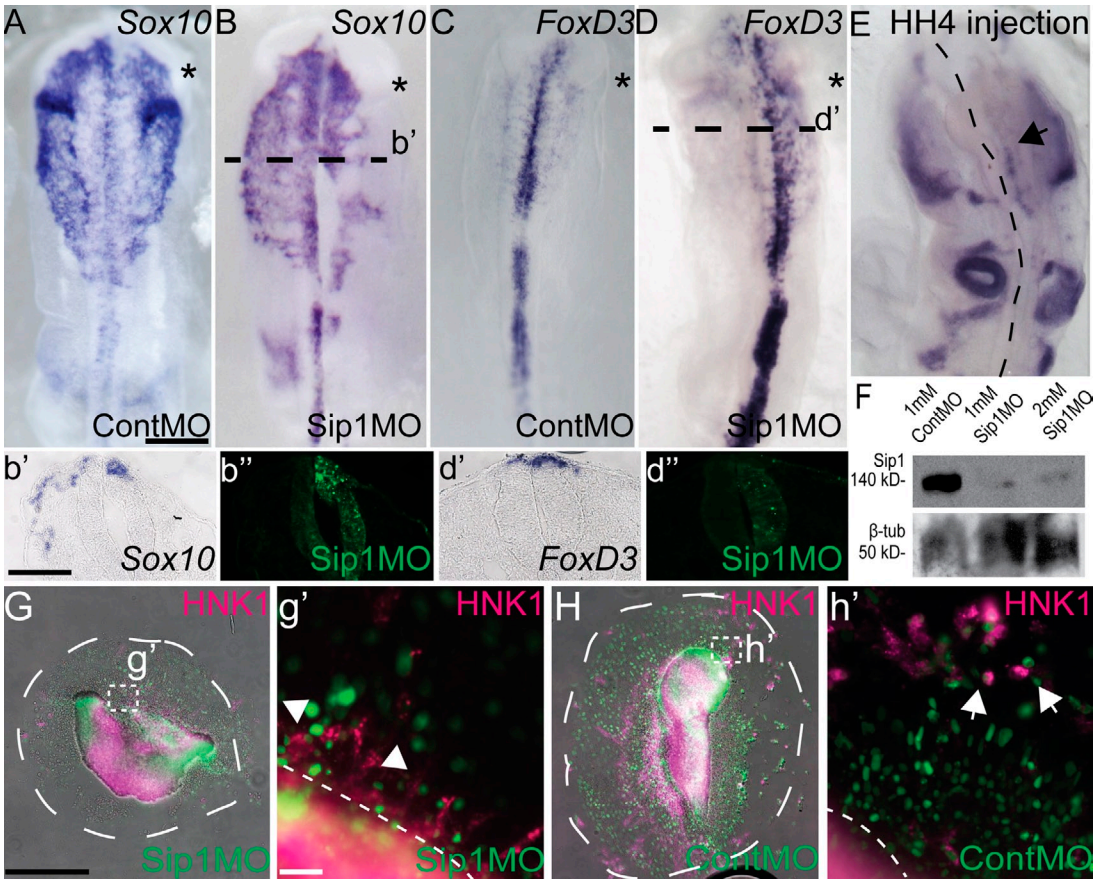

Figure 3. **Loss of Sip1 prevents the completion of neural crest EMT.** Whole-mount in situ hybridization of embryos electroporated with ContMO (A and C) or Sip1MO (B and D) at HH4 and collected at HH10. A and B, *Sox10* expression; C and D, *FoxD3* expression. While ContMO-electroporated embryos have normal expression of both genes, Sip1-electroporated embryos exhibit decreased expression of (B) *Sox10* in the migratory crest (n = 11/13) and aberrantly maintain (D) *FoxD3* in the dorsal neural tube (n = 7/10). (b'–d'') Sections from levels indicated by dotted lines in B and D. (E) In situ hybridization for *Sox10* on an HH13 embryo electroporated at HH4 with Sip1MO showing a maintenance of neural crest near the midline at the level of the midbrain (asterisk; n = 4/5). (F) Western blot analysis of Sip1 protein expression in HH9–10 embryos after injection of 1 mM ContMO, 1 mM Sip1MO, and 2 mM Sip1MO showing that Sip1 protein expression is greatly reduced after Sip1MO electroporation. The data shown here are representative of one experiment out of three repeats. In this experiment, protein was pooled from 8–10 chicken whole embryos. (G and H) Whole-mount immunohistochemistry for HNK1 (magnification of 10) comparing neural tube explants from embryos electroporated with either (G) Sip1MO (n = 8/8) or (H) ContMO (n = 6/6) showing lack of migration and clumping phenotype. Dashed lines indicate distance migrated by furthest cells from the explant. Explants are overlaid with bright-field images. (g' and h') A 40× image from dashed box in explants (G and H, respectively) demonstrating HNK1-positive cells that are either clumped outside of the neural tube in Sip1MO-injected explants (g') or that have migrated away from the ContMO-injected explant (h'). (g' and h') High magnification image of explants showing HNK1 expression and Sip1MO or ContMO alone showing that HNK1-positive cells are clumped next to the explant (g', white arrows) or have migrated away from the explant (h', white arrowhead). Bars: (A–E) 200 µm; (b'–d'') 150 µm; (G and H) 100 µm; and (g' and h') 30 µm. The data shown here are from a single representative experiment out of at least three repeats.

The results show that Sip1MO-electroporated cells are able to leave the neural tube and migrate laterally but then tend to aggregate near the midline, likely due to increased cell–cell adhesion (Video 2, asterisks). In comparison to control embryos, these cells maintain more of their cell–cell connections, lose directionality, and fail to migrate far (Videos 1–3; n = 5). The cells exhibit a leading edge (LE), but the LE does not move consistently away from the midline as in ContMO-electroporated cells (Videos 4–6), which are able to separate from the midline, separate from each other, and migrate directionally (Video 4 and Video 5; n = 4). Cell tracking indicated that the cells lacking Sip1 travel a short distance and without proper directionality (Fig. 4 C) when compared with ContMO-injected cells (Fig. 4 G), which migrate linearly and generally laterally away from the embryonic midline. Ultimately, Sip1-depleted NC cells remain adherent to each other (compare Video 3 with Video 6), forming clumps of cells adjacent to the neural tube. This is further evident in a transverse section of an HH9 embryo injected on both sides with membrane plus nuclear RFP and on one side with Sip1MO (Fig. 4, I and J). Whereas NC cells on the control side are spread out (Fig. 4, I and J; left), those on the morpholino-injected side appear stuck together such that it is difficult to distinguish individual cell bodies (Fig. 4, I and J; right, arrows). The inability of the Sip1-depleted cells to detach from each other despite their ability to delaminate and exit from the neural tube suggests that the loss of Sip1 may alter NC cell–cell adhesive behavior in a manner that perturbs their mesenchymalization.

Loss of Sip1 increases E-cadherin levels in the ectoderm and migratory NC

Under normal conditions, expression of adhesion molecules is tightly regulated during EMT. Thus, the observation that Sip1MO-electroporated cells failed to disaggregate raised the

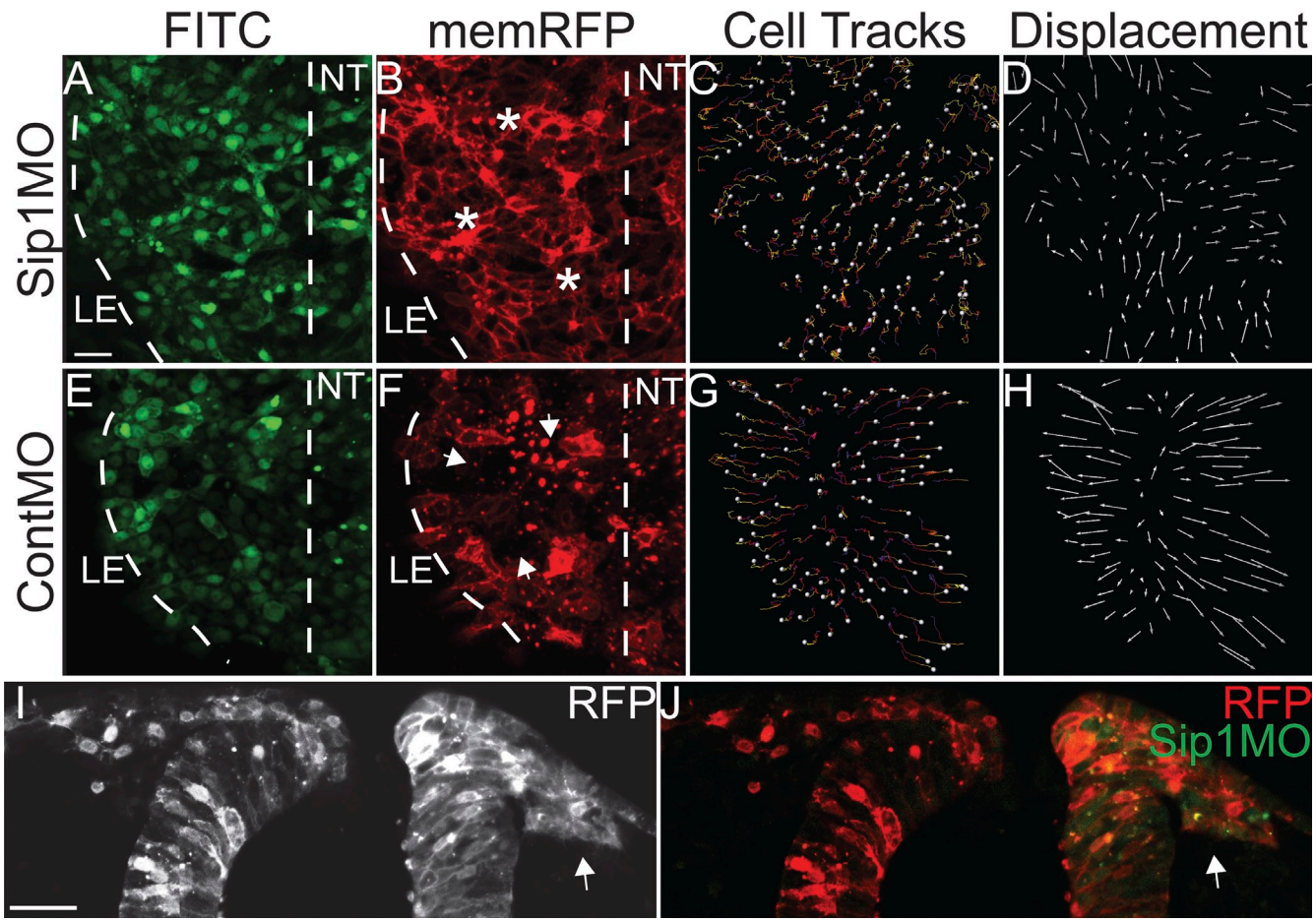

Figure 4. **Neural crest cells lacking Sip1 exhibit reductions in detachment, directional migration, and overall displacement.** Time-lapse imaging of the midbrain regions of living embryos starting at HH10. (A and B) Snapshots of embryos electroporated with Sip1MO-FITC + pCS2-memRFP show electroporated cells that are able to delaminate from the neural tube (NT) and migrate laterally (LE, leading edge). However, they remain connected to each other (asterisks) near the midline and form clumps of cells relative to ContMO-injected cells (E and F). (C and D) Cell tracking and net displacement over time (t = 295 min) shows that Sip1MO-injected cells are unable to migrate long distances away from the midline and in a directional manner as is seen in ContMO embryos (G and H; t = 245 min). (H) Displacement of ContMO-injected cells demonstrates that NC cells near the LE actively migrate away from the midline while the NT appears to move away from the NC cells due to growth and movement. (I and J) Confocal imaging of a histological section from an embryo electroporated on the left side with memRFP + nucRFP and on the right side with Sip1MO + memRFP + nucRFP reveals that Sip1MO-treated cells remain clumped next to the midline (arrows). NT, neural tube; LE, leading edge. (C and G) white dots represent final time points for each track. (A and B) z = 8 µm; (E and F) z = 10 µm; (I and J) z = 6 µm. Bars, 30 µm. See also Videos 1–6. The data shown are representative of multiple repeats (experiment was repeated five [Sip1MO] and four [ContMO] times).

possibility that loss of Sip1 may affect expression of one or more adhesion molecule(s). To test this, we quantitated the effects of Sip1 knockdown on various transcripts, including adhesion molecules, known to be involved in NC development, using the NanoString nCounter system (Fig. 5 A). The results show that the expression of three adhesion molecules was significantly altered by loss of Sip1 (Fig. 5 A; $n = 3$). Whereas *Ecad* expression was up-regulated in cells lacking Sip1, *Ncad* and *cadherin 7* (*Cad7*) were down-regulated. To further verify the effect of Sip1 knockdown on the expression of *Ecad*, we performed quantitative RT-PCR on dissected neural tubes plus adjacent neural crest cells, comparing the ContMO- and Sip1MO-injected sides of the same embryos. The results show that the Sip1MO-injected side expressed *Ecad* at a twofold higher level than the ContMO-injected side (Fig. 5 B; $n = 4$, $P < 0.036$).

To analyze the effect of Sip1 knockdown on Ecad protein expression, we performed Western blot analysis of heads dissected from embryos that were either injected with ContMO or Sip1MO (Fig. 5 C). Consistent with our qPCR results, Ecad protein levels were increased in Sip1MO-injected embryos compared with ContMO embryos. To verify that the *Ecad* transcript levels were up-regulated in the neural tube, we performed whole-mount in situ hybridization using an *Ecad* probe. Embryos injected with Sip1MO exhibited a strong up-regulation of *Ecad* expression in the neural tube compared with the contralateral side (Fig. 5 D; $n = 8/10$). Next, we performed immunohistochemistry to localize Ecad protein after Sip1MO knockdown. To this end, ContMO was electroporated into the left side of HH4 embryos, concurrent with the electroporation of Sip1MO into the right side of the same embryo. There was a marked up-regulation of Ecad protein expression in both the ectoderm and the migratory

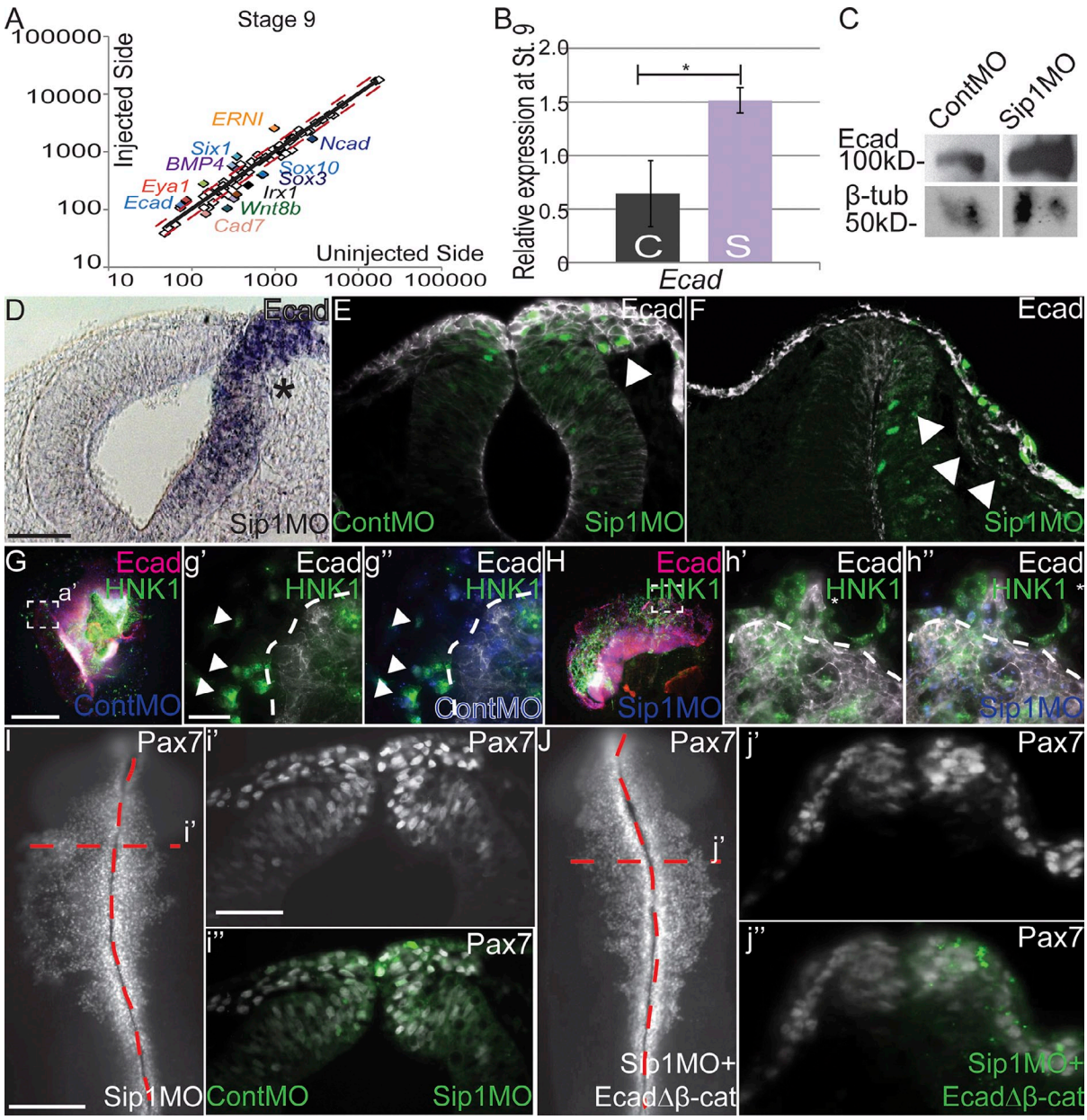

Figure 5. **Sip1 knockdown leads to maintenance of Ecad protein in migratory NC cells.** (A) Multiplex NanoString analysis of transcripts from neural tubes dissected from HH9 embryos, comparing the Sip1MO electroporated side to the control side of the same embryo. The results show that *Ecad* mRNA levels are up-regulated while *Ncad* and *Cad7* are reduced ($n = 3$). The data shown here are representative of three separate experiments with the changes in transcript data pooled. (B) Quantitative RT-PCR analysis of neural tubes plus migratory crest cells dissected from HH9 embryos that were electroporated on the left side with ContMO (C) and on the right side with Sip1MO (S) at HH4. *Ecad* gene expression was compared with GAPDH expression. Error bars are standard deviation between samples and $P < 0.036$ (asterisk indicates statistical significance; $n = 4$). The data shown here are one representative experiment with expression data from four embryos, and this was repeated four times. (C) Western blot analysis of Ecad protein expression after the injection of 1 mM ContMO and 1 mM Sip1MO showing that Ecad protein expression is increased after Sip1MO electroporation. The data shown here are representative of one experiment out of three repeats. In this experiment, protein was pooled from 8–10 chicken whole embryos. β-Tubulin was used as a loading control. (D) In situ hybridization using a probe for *Ecad* shows that it is ectopically expressed in the neural tube after Sip1 knockdown (asterisk). Embryo injected on right side as indicated by asterisk. (E and F) Whole-mount immunohistochemistry for Ecad in midbrain sections at 40× in HH9 (E) and HH15 (F) embryos demonstrates increased sequestration of Ecad protein on the cell membranes on the Sip1MO side compared with the control side (white arrowheads). (G and H) To visualize the change in Ecad protein expression in vitro, neural tubes were dissected from HH8 embryos electroporated with ContMO on the left side and Sip1MO on the right side at HH4. Explants were cultured for 12–24 h and examined for expression of Ecad and HNK1. (G) ContMO-injected migratory neural crest cells express HNK1 (green) but lack Ecad expression (g′, white arrows), whereas cells lacking Sip1 (H) emigrate from the neural tube explants (marked by white dashed line) but fail to detach from each other or migrate far from the explant ($n = 6/8$). Additionally, the Sip1MO-injected cells co-express HNK1 (green) and Ecad protein (h′, white asterisk), suggesting that delamination from the neural tube explant does not require Ecad down-regulation, whereas subsequent detachment and migration does. (I and J) Whole-mount immunohistochemistry using an antibody for Pax7 in embryos electroporated with (I) ContMO on the left and Sip1 on the right (less migration on right) and (J) Sip1MO + EcadΔβcatenin on the right (recovered migration). Red dashed lines indicate midline and level of section. (i′) A section through the embryo in panel I demonstrating clumped Pax7-positive cells on the Sip1MO-injected side. (i′′) An overlay of Pax7 and FITC from ContMO and Sip1MO. (j′) A section of the embryo from J demonstrating recovered Pax7-positive cells on the Sip1MO + EcadΔβ-catenin–injected side. (j′′) An overlay of Pax7 and FITC Sip1MO. Bars: (D–J) 100 μm; (g′–h′′) 30 μm; (i′–j′′) 50 μm. The whole-mount and section data shown here are from a single representative experiment out of at least three repeats.

NC cells on the Sip1MO side compared with the control side of the same embryo (Fig. 5 E; n = 26/30). Cells lacking Sip1 appeared to maintain expression of Ecad on all surfaces, consistent with the observed increase in cell–cell adhesion and rounded cellular morphology. This phenotype was observed in older embryos as well (Fig. 5 F; n = 4/5). As late as HH12–13, these cells maintained high levels of Ecad protein and remained connected to one another. In neural tube explants (Fig. 5, G and H), ContMO NC cells emigrated out of the neural tube explant and down-regulated Ecad protein in migratory cells that expressed the HNK1 epitope (Fig. 5 g′). However, cells lacking Sip1 remained close to the neural tube, failed to become mesenchymal (Fig. 5, H and h′), and maintained Ecad protein expression while expressing HNK1 (Fig. 5 h′).

Because of the observed reciprocal relationship between Sip1 and Ecad, we predicted that simultaneous knockdown of both Sip1 and Ecad might rescue the phenotype. To test this possibility, we co-electroporated Sip1MO while blocking Ecad function via a dominant-negative form of human Ecad that lacks the β-catenin binding domain (EcadΔβ-cat) (Gottardi et al., 2001). Embryos were injected with (1) ContMO on the left side and Sip1MO on the right side (Fig. 5 I) or (2) Sip1MO + EcadΔβ-cat on the right side (Fig. 5 J). The resultant phenotypes were characterized using antibodies against Pax7 (Fig. 5, I and J) and Snail2 (not depicted), which are expressed in the nuclei of premigratory and migrating cranial NC cells. As expected, Sip1 knockdown resulted in a failure of NC cells to move far from the neural tube (Fig. 5, I and i′; n = 13/17, right side) when compared with the ContMO-injected side. In contrast, co-electroporation of Sip1MO + EcadΔβ-cat was able to partially rescue the Sip1MO phenotype (Fig. 5, J and j′; n = 10/13), with the Pax7-positive migratory cells emigrating earlier and farther from the neural tube. These findings support an epistatic relationship between Sip1 and Ecad.

Sip1 knockdown reduces N-cadherin expression

In addition to Ecad, several other cadherins are expressed at the time of NC emigration, including Cad6B and Ncad (Akitaya and Bronner-Fraser, 1992; Nakagawa and Takeichi, 1998; Coles et al., 2007; Shoval et al., 2007; Dady et al., 2012; Strobl-Mazzulla and Bronner, 2012). Interestingly, we observed a significant decrease in Ncad transcript and protein expression in the dorsal neural tube after Sip1 knockdown. This reduction was confirmed by qPCR (Fig. 6 A; n = 4, P = 0.046), Western blot analysis (Fig. 6 B), whole-mount in situ hybridization (Fig. 6 C, inset; n = 16/19) and immunohistochemistry (Fig. 6 D; n = 21/23). Each assay revealed a decrease in Ncad expression on the Sip1MO-injected side compared with the ContMO or uninjected side of the same embryo. In contrast, loss of Sip1 protein did not increase Cad6B gene or protein expression at midbrain levels, but did somewhat delay the expression of *Cad6B* transcript without significantly affecting protein levels (Fig. S3).

Finally, we tested if concurrently knocking down Sip1 and overexpressing full-length chicken Ncad (Shiau and Bronner-Fraser, 2009) at HH4 would rescue the loss-of-function phenotype. Whereas Sip1MO alone caused a decrease in neural crest migration as analyzed by Snail2 expression (Fig. 6, E–e′′; n = 12/14), Sip1MO + Ncad led to a partial rescue of NC migratory ability, demonstrated by similar numbers and migratory ability of Snail2+ cells on experimental and control sides (Fig. 6, F–f′′). However, the addition of exogenous Ncad failed to completely restore the mesenchymal morphology of NC cells, and the Snail2+ migratory NC cells remained clumped together on the injected but not the uninjected side (Fig. 6, f′ and f′′; n = 10/14). Co-expression of Ncad appears to decrease the levels of Ecad protein in the Sip1MO-injected cells, thus partially restoring normal Ecad protein levels in the premigratory cells (Fig. 6, G and H; n = 8/11), perhaps explaining its ability to rescue the phenotype.

Discussion

Numerous EMT factors have been implicated in cell transformation and metastasis in various types of cancer (Kang and Massagué, 2004; Thiery et al., 2009; Kerosuo and Bronner-Fraser, 2012). For example, the Sip1/Zeb, Snail, and Twist transcription factor families are highly linked to tumor metastasis (Sánchez-Tilló et al., 2012). However, much less is known about the role of these EMT factors in vivo during embryonic EMTs. Moreover, the same transcription factors appear to have divergent functions in different vertebrates, highlighting the need for better clarification of the molecular pathways driving developmental EMT.

During embryogenesis, Sip1 functions at multiple time points and in varied processes that are seemingly unrelated to EMT. The N terminus zinc-finger domain is required for neural induction in frog embryos (Eisaki et al., 2000; van Grunsven et al., 2000; Sheng et al., 2003), whereas the C terminus zinc finger domain is required for repression of *Xenopus brachyury* (*Xbra/Tbx6*) to maintain the separation of neural and mesodermal tissues (Sheng et al., 2003; Nitta et al., 2007). Sip1 is also required for normal anterior–posterior patterning in zebrafish (Delalande et al., 2008). It has also been linked to the regulation of adhesion molecules during EMT in the heart, and appears to be regulated by olfactomedin-1 for cell invasion (Lencinas et al., 2013). At later stages, dysregulated Sip1 has been associated with the vagal neurocristopathies, Mowat-Wilson syndrome and Hirschsprung's disease (Wakamatsu et al., 2001).

Adding to its developmental functions, the present study shows that Sip1 is required for cranial NC cells to complete the process of EMT. Our results also highlight that there are at least two discrete steps required for the process of cranial neural crest EMT: detachment from the neural tube and subsequent separation of NC cells from the epidermis and each other. After loss of Sip1, NC cells are able to complete the first step but not the second. Although they exit the neural tube, they remain rounded and clumped together outside of the neural tube and are unable to detach from each other, preventing the rearrangements that are required to navigate through the ECM. This phenotype is likely due to increased expression of Ecad in the epidermis and migratory NC cells and the concomitant decrease in Ncad in the neural tube and therefore in the migratory crest cells (Fig. 7). These data suggest that the

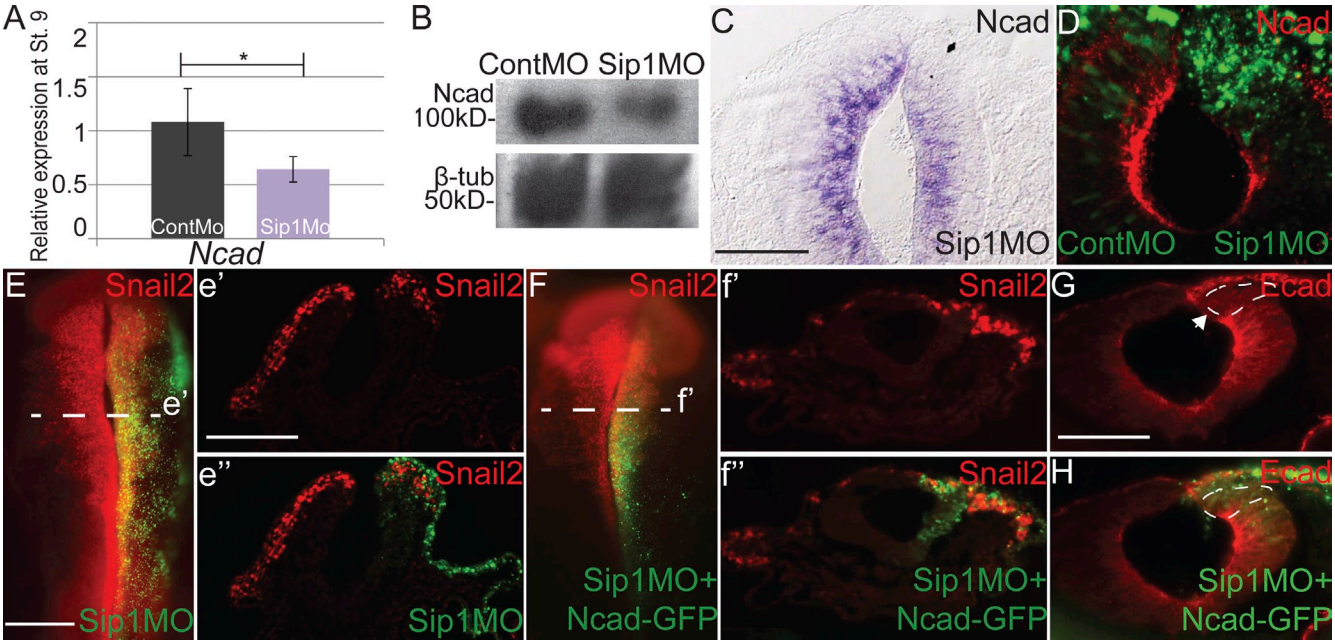

Figure 6. **Ncad expression is reduced in cells lacking Sip1.** (A) Quantitative PCR analysis of neural tubes and migratory crest cells dissected from HH9 embryos that were electroporated on the left side with ContMO and on the right side with Sip1MO at HH4. *Ncad* expression was compared with GAPDH expression. Error bars are standard deviation between samples and $P < 0.046$ ($n = 4$). The data shown here are one representative experiment with expression data from four embryos, and this was repeated four times. Asterisk indicates statistical significance. (B) Western blot analysis of Ncad protein expression after the injection of 1 mM ContMO and 1 mM Sip1MO showing that Ncad protein expression is decreased after Sip1MO electroporation. β-Tubulin was used as a loading control. The data shown here are representative of one experiment out of two repeats. In this experiment, protein was pooled from 8–10 chicken whole embryos. (C) Whole-mount in situ hybridization for *Ncad* expression in embryos lacking Sip1 on the right side shows a decrease in *Ncad*. (D) Confocal image of a section from an embryo, electroporated with ContMO on the left side and Sip1MO (green) on the right side, showing decrease in Ncad protein (red) expression (Z = 8 µm). (E and F) Whole-mount immunohistochemistry using an antibody for Snail2 of an embryo electroporated with (E) Sip1MO on the right side or (F) Sip1MO + *Ncad-GFP* DNA on the right side. Snail2 expression is reduced in the Sip1MO-injected cells, and this effect is rescued by co-electroporation of Sip1MO + *Ncad-GFP* cells. (e′) A section from the embryo in E showing loss of Snail2 protein. (e′′) Overlay of Snail2 and Sip1MO. (f′) A section from the embryo in F at the level indicated by dashed white line shows that although Snail2 appears reduced in whole mount, Snail2 expression and numbers of migratory NC cells are partially rescued. (G) Whole-mount immunohistochemistry using an antibody to Ecad on an embryo electroporated with Sip1MO + *Ncad-GFP* DNA on the right side shows that although Ecad protein is still increased on the injected side, it is at a lower level in the cells injected with high levels of Ncad-GFP and Sip1MO (indicated by dashed circle and white arrow) than with Sip1MO alone. Bars: (C and D) 30 µm; (E and F) 200 µm; (e′ and f′) 100 µm; and (G and H) 50 µm. The whole-mount and section data shown here are from a single representative experiment out of at least three repeats.

switch between Ecad and Ncad in NC cells likely plays a critical role in completing EMT and creating functionally motile, mesenchymal NC cells.

Sip1 is required to reduce Ecad in migratory NC cells

The expression of adhesion molecules undergoes a well-documented transition that appears to be tightly regulated to allow for normal neural crest EMT (Kerosuo and Bronner-Fraser, 2012). It was previously thought that Ncad and Cad6B were the two most critical adhesion molecules involved in neural crest EMT; both are expressed at the onset of EMT and are down-regulated in the dorsal neural tube, facilitating cranial neural crest detachment from the neural tube (Nakagawa and Takeichi, 1998). Furthermore, maintenance of Cad6B in the dorsal neural tube leads to EMT defects (Coles et al., 2007; Strobl-Mazzulla and Bronner, 2012). In the present study, however, we find that Cad6B is unaffected after Sip1 knockdown (Fig. S3). Instead, Ecad, which is expressed on the apical side of the neural tube epithelium as well as in the early migratory NC (Dady et al., 2012), appears to play a critical role, paralleling the situation in many types of cancer cells (Sivertsen et al., 2006).

Cells lacking Sip1 are able to delaminate from the neural tube but cannot detach from each other, due to an increase in their cell–cell adhesion (Figs. 3 and 4). Our data suggest that Sip1 mediates adhesive changes by regulating Ecad transcript expression and perhaps protein localization in early migratory avian NC cells. Knockdown of Sip1 leads to the up-regulation or maintenance of Ecad transcripts and protein in the epidermis, neural tube, and migratory NC cells in vivo (Fig. 5, A–F). In vitro, Ecad is absent from HNK1+ migrating NC cells in control explants but highly and aberrantly expressed on the cell surface of migrating crest cells after the loss of Sip1 (Fig. 5, G and H). The latter fail to disassociate from each other, preventing the completion of EMT. Sip1 is a well-characterized direct repressor of *Ecad* expression in cancer metastasis and during embryonic development (Comijn et al., 2001; Wakamatsu et al., 2001). However, in early avian development, *Sip1* and *Ecad* transcripts overlap in expression (Dady et al., 2012). Thus, the ability of Sip1 to act as a repressor of *Ecad* expression may be stage-dependent and related to the availability of cofactors that may differ as a function of time. In the mouse, expression of *Sip1* and *Ecad* appear to be mutually exclusive (Wakamatsu et al., 2001). However, in chicken embryos the expression of endogenous

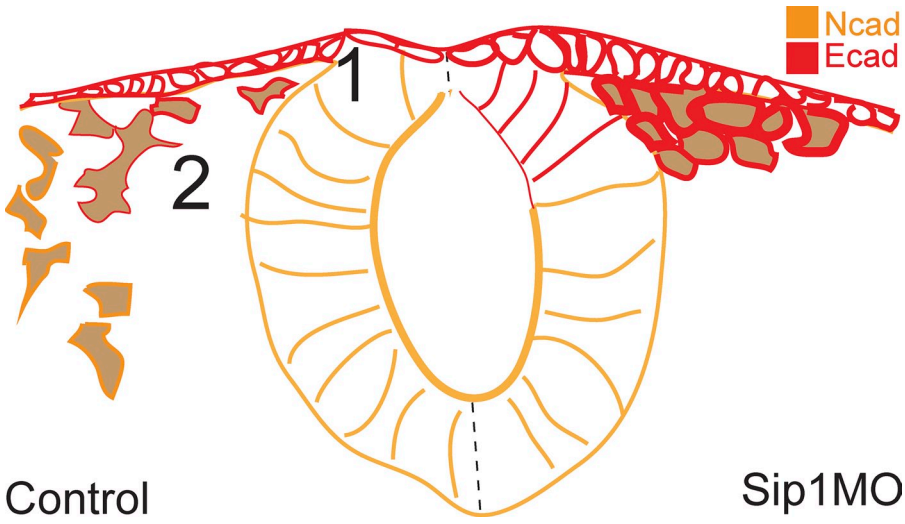

Figure 7. **Diagram showing the effect of Sip1 knockdown on neural crest EMT.** Our results show that NC cells undergoing the process of EMT go through two separate steps to become fully mesenchymal: (1) detachment from the neural tube and (2) separation from the ectoderm and dissociation from the other migratory NC cells. Compared with ContMO or untreated NC cells (left side), loss of Sip1 (right side) has no effect on step 1, but blocks step 2 due to the increased cell–cell adhesion caused by increased Ecad in the neural tube, epidermis, and migratory NC cells (red) and the loss of Ncad expression in the neural tube and migratory NC cells (orange). These data support a critical role for Sip1 in regulation of multiple adhesion molecules during neural crest EMT.

Ecad transcript and protein is maintained in the apical neural tube cells and early migratory crest until approximately HH10–HH11, well after the onset of cranial NC EMT (Dady et al., 2012).

Our results show that NC cells lacking Sip1 maintain a high level of Ecad protein and therefore are unable to migrate normally. However, it is interesting to note that emigrating neural crest cells do normally express some Ecad protein as they leave the neural tube, suggesting a requirement for cell–cell adhesion in the early migrating neural crest cells. During studies of cancer EMT, there is conflicting evidence about the requirement for the down-regulation of adhesion molecules during EMT and metastasis. Recent work by Chui (2013) has suggested that the mesenchymal phenotype of cells does not necessarily confer metastasis; i.e., cancer cells do not need to undergo full EMT to detach from tumors, migrate, and invade other tissues. Our live-imaging studies (compare Video 1 with Video 2) have shown that even in control cells that migrate normally, NC cells appear to migrate as a transient group that is intermittently, but consistently, in contact with the cells that surround them. However, normal neural crest migration requires cell rearrangement to navigate through the ECM and tissues. Our data show that without Sip1, the cells are unable to detach from one another, leading to an inability to complete EMT and navigate through the ECM.

Sip1 is required for Ncad expression

In addition to influencing Ecad levels and distribution, our results suggest that Sip1 influences Ncad expression. Ncad is normally expressed throughout the apical portion of the developing neural tube before NC EMT (Akitaya and Bronner-Fraser, 1992; Nakagawa and Takeichi, 1998). As EMT commences, Ncad is down-regulated in the dorsal neural tube. In addition to the full-length version in the neural tube, there also is a proteolytically cleaved variant of Ncad that is expressed in migratory NC and functions as an EMT activator (Shoval et al., 2007). After loss of Sip1, both *Ncad* transcript and protein expression are decreased (Fig. 6). Despite the excess of Ecad protein that keeps NC cells clumped, it is possible that the observed concomitant excess loss of Ncad allows for their delamination after Sip1 knockdown.

Several possible mechanisms may account for the indirect down-regulation of Ncad after Sip1 loss of function. In addition to its transcriptional role, Sip1 has been shown to inhibit BMP signaling (van Grunsven et al., 2007). In turn, BMP in the dorsal neural tube has been reported to down-regulate Ncad protein (Shoval et al., 2007). Thus, after loss of Sip1, BMP signaling may continue in dorsal neural tube cells, thereby inhibiting Ncad production. Consistent with this possibility, our NanoString data show that *BMP4* transcripts are slightly up-regulated in the dorsal neural tube (Fig. 5 A). A second possibility is that up-regulation of both membrane-bound and cytoplasmic Ecad may lead to a decrease in *Ncad* expression, as has been reported in melanoma cells lines (Kuphal and Bosserhoff, 2006). Finally, the observed maintenance of *FoxD3* expression in the cranial dorsal neural tube (Figs. 2 D and 3 A) may lead to aberrant repression of *Ncad* gene expression. In the trunk NC, which differs from cranial crest in its EMT program, *FoxD3* has been shown to inhibit expression of Ncad while up-regulating integrin β1, laminin, and Cad7 (Cheung et al., 2005). Although these observations were made at a different axial level, our finding that Sip1 up-regulates *FoxD3* but down-regulates *Ncad* is consistent with these previous findings and may suggest that *Sip1* indirectly regulates *Ncad* via FoxD3.

In summary, we show that Sip1, one of the best-characterized cancer EMT-related proteins, is also required for progression of the normal program that regulates neural crest EMT. We find that NC EMT is a two-step process requiring: (1) detachment from the neural tube and (2) a subsequent ability to separate from other NC cells. Sip1 plays a role in the second phase of NC EMT by inversely regulating adhesion molecules Ecad and Ncad in the migratory NC. This switch in cadherins is critical for NC cell EMT and strikingly similar to that observed during cancer metastasis as well as other EMTs such as those during cardiac development (Lencinas et al., 2013). Thus, the key role of Sip1 in regulating transcriptional and potential post-translational events is likely to have significant implications for understanding EMT in both developmental and oncological contexts.

Materials and methods

Embryos
Fertilized chicken eggs were obtained from local commercial sources (McIntyre Farms, San Diego, CA) and incubated at 37°C to the desired stages according to the criteria of Hamburger and Hamilton (HH).

RNA preparation and qPCR
RNA was prepared from individual embryos (n = 3–5) using the RNAqueous-Micro isolation kit (Ambion) following the manufacturer's instructions. The obtained RNA was treated with DNaseI amplification grade (Invitrogen) and then reverse transcribed to cDNA with SuperScript II (Invitrogen) using random hexamers. qPCR was performed using a 96-well plate qPCR machine (ABI 7000; Applied Biosystems) with SYBR Green iTaq Supermix with ROX (Invitrogen), 150–450 nM of each primer, and 200–500 ng of cDNA in a 25-µl reaction volume. During the exponential phase of the qPCR reaction, a threshold cycle (CT) and baseline was set according to the protocols of Applied Biosystems. The results for different samples were then analyzed using the Livak/ΔΔCT method, and the Student's t test was used to determine significance. There were three replicates for every sample and GAPDH was used as a control.

Electroporation of antisense morpholinos and vectors
A translation blocking antisense morpholino to Sip1 (Sip1MO) was designed (5′-CATCCGCCATGATCTGCTGCTTCAT-3′), and one control morpholino (ContMO) was used (5′-CCTCTTACCTCAGTTACAATTTATA-3′). Injections of the fluorescein-tagged morpholinos (0.75–1 mM plus 0.5–1.5 mg/ml of PCI carrier plasmid DNA; Voiculescu et al., 2008) were performed by air pressure using a glass micropipette targeted to the presumptive NC region at HH stages 4–5. Rescue experiments were performed in the same manner as Sip1MO electroporations except that the pCDNA-4/HisMax-hZeb2 (Ellis et al., 2010), pCS2-Ncad-GFP (Shiau and Bronner-Fraser, 2009), and pcDNA3-Ecad-Δβ-catenin (Gottardi et al., 2001) plasmids were used (1 mg/ml) instead of the PCI carrier plasmid. Stage 4–5 electroporations were conducted on whole chick embryo explants placed ventral side up on filter paper rings. The Sip1 morpholino and vectors were injected on the right side of the embryo and the controls were injected on the left side when co-injected, and platinum electrodes were placed vertically across the chick embryos and electroporated with five pulses of 6.3 V in 50 ms at 100-ms intervals. The embryos were cultured in 1.0 ml of albumen in tissue culture dishes until they reached the desired stages. The embryos were then removed and fixed for 20 min to overnight in 4% PFA at room temperature or 4°C, respectively. The embryos were placed in PTW (1× PBS + 0.1% Tween 20), viewed, and photographed as whole mounts using a fluorescence stereomicroscope to show the electroporation efficiency.

Western blot analysis
Western blots were performed to assess whether Sip1 knockdown affected the expression of Sip1, Ncad, and Ecad protein levels. Stage 8–10 chicken embryos were homogenized in a lysis buffer. Protein levels were measured using a Bradford assay and an equal amount of protein was boiled for 10 min and loaded in each lane of an 8% SDS-PAGE gel. The proteins were fractionated by SDS-PAGE and transferred onto nitrocellulose membranes (EMD Millipore). Western blot analysis was performed by using an ECL chemiluminescence blotting kit (GE Healthcare, Boehringer Ingelheim). In brief, after blocking in PBS containing 0.2% Tween and 5% low-fat dry milk for 1 h at room temperature, the membrane was incubated in Sip1, Ncad, Ecad, or β-tubulin antibody, followed by development using ECL chemiluminescence reagents and visualization by x-ray autoradiography.

NanoString nCounter
Individual halves of embryo neural tubes treated with Sip1-MO were disaggregated in lysis buffer (Ambion) and stored at −80°C. The total RNA from the lysates was then allowed to hybridize with the capture and reporter probes incubating overnight at 65°C according to the nCounter gene expression assay manual. After the washes, the purified target–probe complexes were eluted off and immobilized in the cartridge for data collection performed in the nCounter digital analyzer. Results from three separate embryos were grouped and regression analysis was used to determine differences. Only genes that were altered by 25% or more were considered significant.

In situ hybridization
For whole-mount in situ hybridization, embryos were fixed for 1 h to overnight in 4% paraformaldehyde (PFA) at room temperature or 4°C, respectively, washed in PBS containing 0.1% Tween 20 (PTW), and dehydrated in a MeOH/PTW series at room temperature before being stored at −20°C in 100% MeOH. Chick in situ hybridization was performed as follows: On day 1 embryos were rehydrated in a stepwise manner from 100% MeOH to 100% PBS with 0.1% Tween 20. They were then prehybridized in hybridization buffer (Acloque et al., 2008) for 1 h. The embryos were then hybridized with the digoxigenin-labeled antisense probes overnight at 65–70°C. On day 2 embryos were washed two times for 30 min in 2× SSC buffer, two times for 30 min in 0.2× SSC buffer, and two times for 10 min in 1× MAB buffer with 0.1% Tween 20 (MABT). Next, embryos were blocked in a solution of 10% BBR and 10% sheep serum in MABT for 1–3 h. The embryos were then incubated with an anti-digoxigenin AP Fab fragments (Roche) in blocking solution for either 3 h at room temperature or overnight at 4°C. Embryos were washed three times for 30 min in MABT and signal was visualized using NBT and BCIP stock solutions (Roche) diluted in alkaline phosphatase buffer and subsequently fixed in 4% paraformaldehyde for 30 min. The linearized plasmid DNA templates that were used for digoxigenin- and fluorescein-labeled RNA probes were *Sip1*, *FoxD3*, *Sox10*, *Ncad*, *Ecad*, *N-Myc*, and *Sox2*. The embryos were imaged in whole mount and after were transverse sectioned at 10–25 µm in a cryostat.

Immunohistochemistry
Immunohistochemistry for Pax7 (Pax7; Developmental Studies Hybridoma Bank [DSHB]), HNK1 (3H5; DSHB), Ncad (MNCD2; DSHB), Cad6B (CCD6B-1; DSHB), Sip1 (ARP39141_P050; Aviva Systems Biology), and Ecad (610181; BD) was performed as follows: embryos were fixed in 4% paraformaldehyde in phosphate buffer for <20 min at room temperature. All washes were performed in TBST + Ca^{2+} + 0.5% Triton X-100. Blocking was performed with 10% donkey serum in the same buffer. The primary antibodies (1:10 for all hybridoma antibodies and 1:1,000 for all others) were incubated in the TBST buffer from overnight to 2 d at 4°C and secondary antibodies (1:500 to 1:1,000) were applied in the same buffer for either 3 h at room temperature or overnight at 4°C.

Live confocal imaging
Embryos were electroporated with 0.75 mM ContMO or Sip1MO (FITC labeled) + 1.5 mg/ml membrane RFP and/or nuclear RFP. They were imaged in the Lab-Tek chambered 1.0 borosilicate coverage glass system (Thermo Fisher Scientific) coated with <0.5 ml 0.6% low-melt agarose mixed with Ringer's solution. Embryos were maintained at 37°C during imaging. A confocal microscope (LSM 510 Meta or LSM 710; Carl Zeiss) was used with an LD C-Apochromat 40×/1.1 W Corr objective (Carl Zeiss). Time lapses were done with a z_{total} = ∼31 µm to leave space for z-drift. Time points were collected at 5-min intervals. Subsets in the z-plane containing the cells of interest were selected for clarity. Collected time-lapse data were registered using Imaris software (Bitplane) to account for embryo drift and exported as TIF images and MOV videos. The registration correction (processed with Imaris software) for embryo drift results in the changes in movie shapes seen here. Cell tracking in Imaris was done in the FITC (green) channel. Parameters used included a spot diameter of 5.19 µm and the "Connected Components" algorithm for tracking.

Neural tube explant assays
Neural tube explant assays were performed as follows: embryos were electroporated with 0.75 mM ContMO plus PCI carrier DNA on the left side and 0.75 mM Sip1MO plus PCI carrier DNA on the right side of the same embryo at HH4. Embryos were cultured until HH8 as described previously (Sauka-Spengler and Barembaum, 2008). At HH8, the neural tubes were dissected out of the embryo in Ringer's solution and subsequently placed in in 8-well chamber slides (Sigma-Aldrich) that were coated with 1% fibronectin. The explants were cultured in DMEM with 10% FBS, 2 mM L-glutamine, and 100 units of penicillin with 0.1 mg/ml streptomycin and cultured at 37°C with 0.5% CO_2 from 12–24 h.

Online supplemental material
Fig. S1 shows transcript analyses using NanoString, qPCR, and in situ hybridization; although Sip1MO slightly delays NC specification, the NC cells recover and that neural specification is not affected. Fig. S2 shows whole-mount in situ hybridization for *Sox10* after Sip1MO electroporation at stages HH5, HH6, and HH7 to demonstrate that the loss of Sip1 affects NC development when knocked down as late as HH7. Fig. S3 shows in situ hybridization and whole-mount immunohistochemistry of Cad6B protein to demonstrate that Sip1 knockdown does not affect Cad6B protein expression. Videos 1–3 are live-imaging confocal movies of a chicken midbrain at HH10 after Sip1MO electroporation. Video 1 is Sip1MO-FITC and Video 2 is memRFP. Video 3 shows a 2.3× image of Video 1 to visualize the cell

behavior and morphology. Videos 4–6 are live-imaging confocal movies of a chicken midbrain at HH10 after ContMO electroporation. Video 4 is ContMO-FITC and Video 5 is memRFP. Video 6 shows a 2.3× image of Video 4 to visualize the cell behavior and morphology. Online supplemental material is available at http://www.jcb.org/cgi/content/full/jcb.201305050/DC1.

We would like to thank Tatjana Sauka-Spengler and the Bronner laboratory for helpful discussions. We would also like to thank the Caltech Biological Imaging center where we performed the live-imaging experiments and the Mertz Lab at the University of Wisconsin at Madison for the gift of human *Zeb2* DNA.

This work was supported by National Institutes of Health grant HD037105 (to M.E. Bronner) and a National Institutes of Health minority supplement P01 HD037105 (to C.D. Rogers).

Submitted: 9 May 2013
Accepted: 4 November 2013

References

Acloque, H., D.G. Wilkinson, and M.A. Nieto. 2008. In situ hybridization analysis of chick embryos in whole-mount and tissue sections. *Methods Cell Biol.* 87:169–185. http://dx.doi.org/10.1016/S0091-679X(08)00209-4

Akitaya, T., and M. Bronner-Fraser. 1992. Expression of cell adhesion molecules during initiation and cessation of neural crest cell migration. *Dev. Dyn.* 194:12–20. http://dx.doi.org/10.1002/aja.1001940103

Bildsoe, H., D.A. Loebel, V.J. Jones, A.C. Hor, A.W. Braithwaite, Y.T. Chen, R.R. Behringer, and P.P. Tam. 2013. The mesenchymal architecture of the cranial mesoderm of mouse embryos is disrupted by the loss of Twist1 function. *Dev. Biol.* 374:295–307. http://dx.doi.org/10.1016/j.ydbio.2012.12.004

Bothe, I., M.U. Ahmed, F.L. Winterbottom, G. von Scheven, and S. Dietrich. 2007. Extrinsic versus intrinsic cues in avian paraxial mesoderm patterning and differentiation. *Dev. Dyn.* 236:2397–2409. http://dx.doi.org/10.1002/dvdy.21241

Brabletz, S., and T. Brabletz. 2010. The ZEB/miR-200 feedback loop—a motor of cellular plasticity in development and cancer? *EMBO Rep.* 11:670–677. http://dx.doi.org/10.1038/embor.2010.117

Chen, Y.T., P.O. Akinwunmi, J.M. Deng, O.H. Tam, and R.R. Behringer. 2007. Generation of a Twist1 conditional null allele in the mouse. *Genesis*. 45:588–592. http://dx.doi.org/10.1002/dvg.20332

Chen, Z.F., and R.R. Behringer. 1995. twist is required in head mesenchyme for cranial neural tube morphogenesis. *Genes Dev.* 9:686–699. http://dx.doi.org/10.1101/gad.9.6.686

Cheung, M., M.C. Chaboissier, A. Mynett, E. Hirst, A. Schedl, and J. Briscoe. 2005. The transcriptional control of trunk neural crest induction, survival, and delamination. *Dev. Cell*. 8:179–192. http://dx.doi.org/10.1016/j.devcel.2004.12.010

Chui, M.H. 2013. Insights into cancer metastasis from a clinicopathologic perspective: epithelial-mesenchymal transition is not a necessary step. *Int. J. Cancer.* 132:1487–1495. http://dx.doi.org/10.1002/ijc.27745

Coles, E.G., L.A. Taneyhill, and M. Bronner-Fraser. 2007. A critical role for Cadherin6B in regulating avian neural crest emigration. *Dev. Biol.* 312:533–544. http://dx.doi.org/10.1016/j.ydbio.2007.09.056

Comijn, J., G. Berx, P. Vermassen, K. Verschueren, L. van Grunsven, E. Bruyneel, M. Mareel, D. Huylebroeck, and F. van Roy. 2001. The two-handed E box binding zinc finger protein SIP1 downregulates E-cadherin and induces invasion. *Mol. Cell*. 7:1267–1278. http://dx.doi.org/10.1016/S1097-2765(01)00260-X

Dady, A., C. Blavet, and J.L. Duband. 2012. Timing and kinetics of E- to N-cadherin switch during neurulation in the avian embryo. *Dev. Dyn.* 241:1333–1349. http://dx.doi.org/10.1002/dvdy.23813

Delalande, J.M., M.E. Guyote, C.M. Smith, and I.T. Shepherd. 2008. Zebrafish sip1a and sip1b are essential for normal axial and neural patterning. *Dev. Dyn.* 237:1060–1069. http://dx.doi.org/10.1002/dvdy.21485

Eisaki, A., H. Kuroda, A. Fukui, and M. Asashima. 2000. XSIP1, a member of two-handed zinc finger proteins, induced anterior neural markers in Xenopus laevis animal cap. *Biochem. Biophys. Res. Commun.* 271:151–157. http://dx.doi.org/10.1006/bbrc.2000.2545

Ellis, A.L., Z. Wang, X. Yu, and J.E. Mertz. 2010. Either ZEB1 or ZEB2/SIP1 can play a central role in regulating the Epstein-Barr virus latent-lytic switch in a cell-type-specific manner. *J. Virol.* 84:6139–6152. http://dx.doi.org/10.1128/JVI.02706-09

Gottardi, C.J., E. Wong, and B.M. Gumbiner. 2001. E-cadherin suppresses cellular transformation by inhibiting beta-catenin signaling in an adhesion-independent manner. *J. Cell Biol.* 153:1049–1060. http://dx.doi.org/10.1083/jcb.153.5.1049

Kang, Y., and J. Massagué. 2004. Epithelial-mesenchymal transitions: twist in development and metastasis. *Cell*. 118:277–279. http://dx.doi.org/10.1016/j.cell.2004.07.011

Kerosuo, L., and M. Bronner-Fraser. 2012. What is bad in cancer is good in the embryo: importance of EMT in neural crest development. *Semin. Cell Dev. Biol.* 23:320–332. http://dx.doi.org/10.1016/j.semcdb.2012.03.010

Kuphal, S., and A.K. Bosserhoff. 2006. Influence of the cytoplasmic domain of E-cadherin on endogenous N-cadherin expression in malignant melanoma. *Oncogene*. 25:248–259. http://dx.doi.org/10.1038/sj.onc.1209508

Lander, R., K. Nordin, and C. LaBonne. 2011. The F-box protein Ppa is a common regulator of core EMT factors Twist, Snail, Slug, and Sip1. *J. Cell Biol.* 194:17–25. http://dx.doi.org/10.1083/jcb.201012085

Lander, R., T. Nasr, S.D. Ochoa, K. Nordin, M.S. Prasad, and C. Labonne. 2013. Interactions between Twist and other core epithelial-mesenchymal transition factors are controlled by GSK3-mediated phosphorylation. *Nat Commun*. 4:1542. http://dx.doi.org/10.1038/ncomms2543

Lencinas, A., D.C. Chhun, K.P. Dan, K.D. Ross, E.A. Hoover, P.B. Antin, and R.B. Runyan. 2013. Olfactomedin-1 activity identifies a cell invasion checkpoint during epithelial-mesenchymal transition in the chick embryonic heart. *Dis. Model. Mech.* 6:632–642. http://dx.doi.org/10.1242/dmm.010595

Murray, S.A., K.F. Oram, and T. Gridley. 2007. Multiple functions of Snail family genes during palate development in mice. *Development*. 134:1789–1797. http://dx.doi.org/10.1242/dev.02837

Nakagawa, S., and M. Takeichi. 1998. Neural crest emigration from the neural tube depends on regulated cadherin expression. *Development*. 125:2963–2971.

Nieto, M.A. 2011. The ins and outs of the epithelial to mesenchymal transition in health and disease. *Annu. Rev. Cell Dev. Biol.* 27:347–376. http://dx.doi.org/10.1146/annurev-cellbio-092910-154036

Nieto, M.A., M.G. Sargent, D.G. Wilkinson, and J. Cooke. 1994. Control of cell behavior during vertebrate development by Slug, a zinc finger gene. *Science*. 264:835–839. http://dx.doi.org/10.1126/science.7513443

Nitta, K.R., S. Takahashi, Y. Haramoto, M. Fukuda, K. Tanegashima, Y. Onuma, and M. Asashima. 2007. The N-terminus zinc finger domain of Xenopus SIP1 is important for neural induction, but not for suppression of Xbra expression. *Int. J. Dev. Biol.* 51:321–325. http://dx.doi.org/10.1387/ijdb.062252kn

Sánchez-Tilló, E., Y. Liu, O. de Barrios, L. Siles, L. Fanlo, M. Cuatrecasas, D.S. Darling, D.C. Dean, A. Castells, and A. Postigo. 2012. EMT-activating transcription factors in cancer: beyond EMT and tumor invasiveness. *Cell. Mol. Life Sci.* 69:3429–3456. http://dx.doi.org/10.1007/s00018-012-1122-2

Sauka-Spengler, T., and M. Barembaum. 2008. Gain- and loss-of-function approaches in the chick embryo. *Methods Cell Biol.* 87:237–256. http://dx.doi.org/10.1016/S0091-679X(08)00212-4

Sauka-Spengler, T., D. Meulemans, M. Jones, and M. Bronner-Fraser. 2007. Ancient evolutionary origin of the neural crest gene regulatory network. *Dev. Cell*. 13:405–420. http://dx.doi.org/10.1016/j.devcel.2007.08.005

Sheng, G., M. dos Reis, and C.D. Stern. 2003. Churchill, a zinc finger transcriptional activator, regulates the transition between gastrulation and neurulation. *Cell*. 115:603–613. http://dx.doi.org/10.1016/S0092-8674(03)00927-9

Shiau, C.E., and M. Bronner-Fraser. 2009. N-cadherin acts in concert with Slit1-Robo2 signaling in regulating aggregation of placode-derived cranial sensory neurons. *Development*. 136:4155–4164. http://dx.doi.org/10.1242/dev.034355

Shoval, I., A. Ludwig, and C. Kalcheim. 2007. Antagonistic roles of full-length N-cadherin and its soluble BMP cleavage product in neural crest delamination. *Development*. 134:491–501. http://dx.doi.org/10.1242/dev.02742

Sivertsen, S., R. Hadar, S. Elloul, L. Vintman, C. Bedrossian, R. Reich, and B. Davidson. 2006. Expression of Snail, Slug and Sip1 in malignant mesothelioma effusions is associated with matrix metalloproteinase, but not with cadherin expression. *Lung Cancer*. 54:309–317. http://dx.doi.org/10.1016/j.lungcan.2006.08.010

Strobl-Mazzulla, P.H., and M.E. Bronner. 2012. A PHD12-Snail2 repressive complex epigenetically mediates neural crest epithelial-to-mesenchymal transition. *J. Cell Biol.* 198:999–1010. http://dx.doi.org/10.1083/jcb.201203098

Theveneau, E., L. Marchant, S. Kuriyama, M. Gull, B. Moepps, M. Parsons, and R. Mayor. 2010. Collective chemotaxis requires contact-dependent cell polarity. *Dev. Cell*. 19:39–53. http://dx.doi.org/10.1016/j.devcel.2010.06.012

Thiery, J.P., H. Acloque, R.Y. Huang, and M.A. Nieto. 2009. Epithelial-mesenchymal transitions in development and disease. *Cell*. 139:871–890. http://dx.doi.org/10.1016/j.cell.2009.11.007

van Grunsven, L.A., C. Papin, B. Avalosse, K. Opdecamp, D. Huylebroeck, J.C. Smith, and E.J. Bellefroid. 2000. XSIP1, a Xenopus zinc finger/homeodomain encoding gene highly expressed during early neural development. *Mech. Dev.* 94:189–193. http://dx.doi.org/10.1016/S0925-4773(00)00318-X

van Grunsven, L.A., V. Taelman, C. Michiels, G. Verstappen, J. Souopgui, M. Nichane, E. Moens, K. Opdecamp, J. Vanhomwegen, S. Kricha, et al. 2007. XSip1 neuralizing activity involves the co-repressor CtBP and

occurs through BMP dependent and independent mechanisms. *Dev. Biol.* 306:34–49. http://dx.doi.org/10.1016/j.ydbio.2007.02.045

Verschueren, K., J.E. Remacle, C. Collart, H. Kraft, B.S. Baker, P. Tylzanowski, L. Nelles, G. Wuytens, M.T. Su, R. Bodmer, et al. 1999. SIP1, a novel zinc finger/homeodomain repressor, interacts with Smad proteins and binds to 5′-CACCT sequences in candidate target genes. *J. Biol. Chem.* 274:20489–20498. http://dx.doi.org/10.1074/jbc.274.29.20489

Voiculescu, O., C. Papanayotou, and C.D. Stern. 2008. Spatially and temporally controlled electroporation of early chick embryos. *Nat. Protoc.* 3:419–426. http://dx.doi.org/10.1038/nprot.2008.10

Wakamatsu, N., Y. Yamada, K. Yamada, T. Ono, N. Nomura, H. Taniguchi, H. Kitoh, N. Mutoh, T. Yamanaka, K. Mushiake, et al. 2001. Mutations in SIP1, encoding Smad interacting protein-1, cause a form of Hirschsprung disease. *Nat. Genet.* 27:369–370. http://dx.doi.org/10.1038/86860

Zhang, C., and M.W. Klymkowsky. 2009. Unexpected functional redundancy between Twist and Slug (Snail2) and their feedback regulation of NF-kappaB via Nodal and Cerberus. *Dev. Biol.* 331:340–349. http://dx.doi.org/10.1016/j.ydbio.2009.04.016